Phys Chem Minerals (1993) 19:361–368

PHYSICS AND CHEMISTRY OF MINERALS

The Effect of Fe on the Crystal Structure of Wadsleyite β-$(Mg_{1-x}Fe_x)_2SiO_4$, $0.00 \leq x \leq 0.40$

Larry W. Finger[1], Robert M. Hazen[1], Jinmin Zhang[1], Jaidong Ko[2], and Alexandra Navrotsky[3]

1 Geophysical Laboratory, Carnegie Institution of Washington, Washington, DC 20015-1305, USA
[2] Department of Earth and Space Sciences, State University of New York, Stony Brook, NY 11794, USA
[3] Department of Geological and Geophysical Sciences, Princeton University, Princeton, NJ 08544, USA

Received December 3, 1991 / Revised, accepted July 1, 1992

Abstract. Single crystals of five wadsleyite compositions, β-$(Mg,Fe)_2SiO_4$ with $Fe/(Fe+Mg)=0.00$, 0.08, 0.16, 0.25 and 0.40, have been synthesized at high temperature and pressure in a uniaxial, split-sphere apparatus. Crystal structures of these samples, determined by x-ray diffraction techniques, reveal that iron is significantly ordered: Fe is depleted in the M2 octahedron, while it is enriched in M1 and M3. The most iron-rich synthetic sample, which falls well outside previous estimates of wadsleyite stability, raises questions regarding published $Mg_2SiO_4-Fe_2SiO_4$ phase diagrams at transition zone conditions.

Introduction

The structure and crystal chemistry of wadsleyite, the β form of $(Mg,Fe)_2SiO_4$, is of interest to mineralogists and seismologists because the $\alpha \rightarrow \beta$ phase transition occurs at pressure-temperature conditions comparable to those of the 400 km discontinuity (Fei et al. 1991). Ringwood and Major (1966) first noted a phase intermediate between olivine (α) and spinel (γ) in low-iron compositions. The crystal structure of this β-phase was solved by Morimoto et al. (1969) for a single crystal of Mn_2GeO_4, and by Moore and Smith (1970) for a powdered sample of $(Mg_{0.9}Ni_{0.1})_2SiO_4$. Horiuchi and Sawamoto (1981) refined the structure of β-Mg_2SiO_4 from single crystals grown at 2000° C, 18.5 GPa in a multi-anvil high-pressure device. From Pauling bond strengths and calculated electrostatic potentials, Smyth (1987) concluded that O1 is substantially underbonded and that it could be replaced by a hydroxyl, if charge balance were maintained by partial M-site vacancy. Downs (1989) used the diffraction data of Horiuchi and Sawamoto (1981) to derive an experimental electrostatic potential and found a minimum in this function close to O2, not O1 as suggested by Smyth.

The present study has been undertaken to investigate changes in crystal chemistry of wadsleyite as a function of iron content and to attempt to detect structural reasons for the limited solid substitution of Fe for Mg. These structural studies will also serve as baseline data for a series of high-pressure crystallographic studies now in progress. In addition, we report the unexpected synthesis of wadsleyite crystals with $Fe/(Fe+Mg)=0.40$, significantly more iron rich than previously observed.

Experimental

Crystals of iron-bearing β-phase, grown in the uniaxial, split-sphere apparatus (USSA-2000) at the Stony Brook High-Pressure Laboratory under the synthesis conditions listed in Table 1, were selected for crystallographic study. Samples with compositions of 0.00, 0.08, 0.16 and 0.25 for $Fe/(Fe+Mg)$ were synthesized specifically for this study, as well as for investigations on wadsleyite compressibility (Hazen et al. 1990) and high-pressure crystal chemistry (in progress). We used dried and powdered mixtures of forsterite and fayalite as starting materials. Compositions were confirmed with electron microprobe analysis.

Optical examination revealed all samples to be inclusion free and uniform in color, with pronounced pale green-to-dark blue green pleochroism in the iron-bearing samples. Spindle stage techniques were employed to determine refractive indices of the 0-, 8- and 16%-Fe wadsleyite samples (the 25% iron specimen is too dark to make refractive index measurements). Values of $N_p=1.696$, $N_m=1.700$, and $N_g=1.705$ are observed for the iron-free sample. For 8%-Fe indices increase to 1.705, 1.713, and 1.720, while those for 16%-Fe are 1.725, 1.730, and 1.735 (all indices ± 0.005).

Mössbauer spectroscopy of the 16%-Fe sample were performed by Y. Fei, who observed ferric iron as approximately 6% of total iron. Such small amounts of Fe^{3+} are typical of many synthetic ferrous iron silicates (Y. Fei, personal communication).

In addition, an unexpected wadsleyite sample with composition $(Mg_{0.6}Fe_{0.4})_2SiO_4$ was obtained from a 3 h run (SUNY 1029) at 15.2 GPa and 1700° C, presumably well within the stability field of silicate spinel, γ-$(Mg,Fe)_2SiO_4$ (Fig. 1). Electron microprobe analysis of five crystals in this run reveal a uniform composition: $Fe/(Fe+Mg)=0.395\pm0.009$, significantly greater than the previously assumed ≈ 0.25 maximum iron content for wadsleyite. Crystals up to 150 μm in diameter are optically opaque in all but thin edges (<15 μm thick), which appear dark green in transmitted light. Mössbauer spectroscopy of this sample (Y. Fei, personal communications) reveals less than 5% of total iron as Fe^{3+}.

Table 1. Crystallographic data for iron-bearing wadsleyite

Parameter	Fe00	Fe08	Fe16	Fe25	Fe40
Synthesis conditions					
P, GPa	16.0	16.5	14.5	15.5	15.2
T, °C	1400	1800	1800	1800	1700
Time, hr	1	4	3	3	3
Capsule	Pt	Re	Re	Re	Re
Unit-cell parameters					
a, Å	5.6921 (2)[a]	5.7037 (9)	5.7119 (9)	5.717 (1)	5.739 (2)
b, Å	11.460 (1)	11.4529 (8)	11.4681 (8)	11.506 (1)	11.515 (2)
c, Å	8.253 (2)	8.2679 (9)	8.2799 (9)	8.299 (1)	8.316 (1)
V, Å^3	538.3 (2)	540.1 (1)	542.4 (1)	545.9 (2)	549.6 (2)
ρx, g cm^{-3}	3.472 (1)	3.585 (1)	3.693 (1)	3.807 (1)	4.010 (1)
Absorption correction					
μ_l, cm^{-1}	11.1	19.0	26.8	35.4	49.8
Size, mm	0.06 × 0.12 × 0.13	0.04 × 0.09 × 0.09	0.04 × 0.10 × 0.13	0.03 × 0.09 × 0.10	0.03 × 0.06 × 0.10
$T_{min}-T_{max}$[b]	0.88–0.94	0.84–0.91	0.78–0.90	0.72–0.83	0.70–0.81
Residuals					
R_{int}[c]	0.018	0.024	0.025	0.026	0.062
Number	452	452	455	456	462
R_w[a]	0.015	0.018	0.018	0.024	0.016
R[e]	0.022	0.029	0.028	0.037	0.032
No. Obs.	399	390	397	379	405
R_w	0.015	0.018	0.018	0.023	0.016
R	0.015	0.021	0.020	0.027	0.024
GOF[f]	0.77	0.74	0.71	0.93	1.14

[a] Numbers in parentheses are the estimated standard deviation in the last quoted decimal place. This conventional is followed in all subsequent tables

[b] T is transmission factor

[c] R_{int} is residual for internal agreement of symmetry equivalent reflections

[d] $R_w=(\Sigma w(F_o-F_c)^2/\Sigma wF_o^2)^{0.5}$

[e] $R=\Sigma||F_o-F_c||/\Sigma|F_o|$

[f] $GOF=\Sigma w(F_o-F_c)^2/(n-m)$, where n is the number of observations and m is the number of parameters

Samples of each material, selected by their defect-free optical appearance, were mounted on a Rigaku AFC-5R single-crystal X-ray diffractometer operated at 45 kV, 180 ma. A search routine located the positions of 20 reflections for automatic indexing. All observed diffraction maxima had reasonable shapes; furthermore, none indicated any twinning or other types of intergrowths. The positions of 25 reflections between 50 and 60° 2θ were used to refine the orientation matrices and lattice constants. The latter quantities, adjusted according to orthorhombic constraints as described by Ralph and Finger (1982), are listed in Table 1, along with calculated densities. The extinction symbol is *I*--(*ab*), consistent with space groups *Im2a, I2mb, Immb, or Imma*. As shown in previous studies, the last choice is correct.

A hemisphere of intensity data was measured for each crystal to sin $\theta/\lambda \leq 0.705$ Å^{-1} for Mo Kα_1 radiation ($\lambda=0.7093$ Å). The instrument was operated with step scans of $\pm 0.75°$ on ω, a step size of 0.03°, and an effective scan rate of 2°/minute. Integrated intensities were calculated with the Lehmann and Larsen (1974) algorithm and converted to structure factors by correction for geometric factors and absorption using a program modified from that of Burnham (1966). Average structure factors were calculated by averaging the symmetry equivalent reflections in Laue group *mmm*. Table 1 also lists linear absorption coefficients, crystal sizes, range of transmission factors, and the internal agreement of the reflection averaging process, which ranges from 0.018 to 0.026 for the five crystals and gives a measure of the residual expected in the crystal structure refinement.

Crystal structure refinements were accomplished with programm RFINE4 (Finger and Prince 1975) using complex scattering factors for neutral atoms (International Tables of Crystallography,

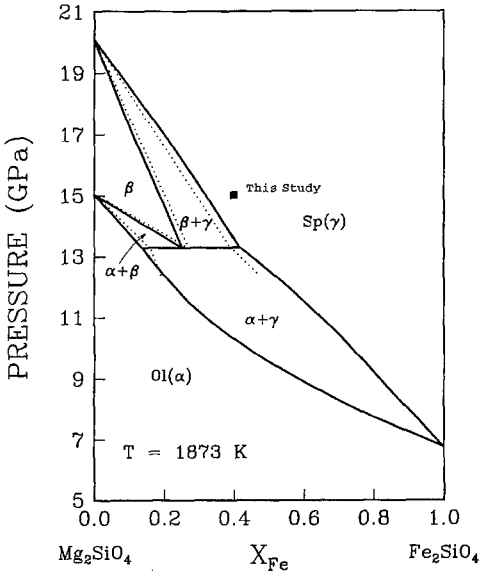

Fig. 1. The $Mg_2SiO_4-Fe_2SiO_4$ isothermal (1600° C) phase diagram, after Fei et al. (1991), with experimental phase boundaries (*dotted lines*) by Katsura and Ito (1989). The fields designated α, β, and γ correspond to olivine, wadsleyite, and silicate spinel orthosilicate structures. The synthesis conditions of wadsleyite (β) crystals with Fe/(Fe+Mg)=0.40 are indicated by the square. Note that this sample lies well within the silicate spinel (γ) stability field

Table 2. Positional and equivalent isotropic thermal parameters for iron-bearing wadsleyite

Parameter	Fe00	Fe08	Fe16	Fe25	Fe40
Extn. Coef(10^{-4})	0.106 (7)	0	0.001 (5)	0.017 (6)	0.000 (3)
M1, Fe Occ	0.0	0.083 (3)	0.171 (3)	0.288 (4)	0.443 (4)
x, y, z	0	0	0	0	0
B	0.47 (1)	0.50 (2)	0.50 (2)	0.63 (3)	0.68 (2)
M2, Fe Occ	0.0	0.039 (3)	0.085 (3)	0.132 (4)	0.234 (4)
x	0	0	0	0	0
y	1/4	1/4	1/4	1/4	1/4
z	0.97013 (8)	0.97051 (11)	0.97049 (11)	0.97069 (14)	0.97069 (12)
B	0.37 (1)	0.45 (2)	0.50 (2)	0.57 (3)	0.77 (3)
M3, Fe, Occ	0.0	0.099 (3)	0.192 (3)	0.290 (4)	0.461 (4)
x	1/4	1/4	1/4	1/4	1/4
y	0.12636 (4)	0.12654 (6)	0.12603 (5)	0.12530 (6)	0.12490 (5)
z	1/4	1/4	1/4	1/4	1/4
B	0.55 (1)	0.54 (2)	0.54 (1)	0.65 (2)	0.82 (1)
Si, x	0	0	0	0	0
y	0.12008 (2)	0.12023 (4)	0.12042 (4)	0.12079 (6)	0.12107 (6)
z	0.61659 (3)	0.61667 (6)	0.61670 (5)	0.61665 (8)	0.61621 (8)
B	0.27 (1)	0.33 (1)	0.28 (1)	0.33 (1)	0.32 (1)
O1, x	0	0	0	0	0
y	1/4	1/4	1/4	1/4	1/4
z	0.2187 (1)	0.2169 (2)	0.2174 (2)	0.2179 (3)	0.2185 (3)
B	0.41 (2)	0.48 (3)	0.47 (3)	0.53 (4)	0.62 (4)
O2, x	0	0	0	0	0
y	1/4	1/4	1/4	1/4	1/4
z	0.7168 (1)	0.7166 (2)	0.7167 (2)	0.7164 (3)	0.7168 (3)
B	0.39 (2)	0.48 (3)	0.40 (3)	0.46 (4)	0.54 (4)
O3, x	0	0	0	0	0
y	0.98946 (8)	0.9894 (1)	0.9889 (1)	0.9879 (2)	0.9878 (2)
z	0.25562 (10)	0.2559 (2)	0.2561 (2)	0.2564 (2)	0.2568 (2)
B	0.42 (2)	0.45 (3)	0.46 (2)	0.52 (4)	0.58 (3)
O4, x	0.2608 (1)	0.2610 (2)	0.2621 (2)	0.2619 (2)	0.2626 (2)
y	0.12286 (4)	0.12280 (9)	0.12293 (9)	0.1230 (1)	0.1234 (1)
z	0.99291 (7)	0.9923 (1)	0.9924 (1)	0.9924 (1)	0.9926 (1)
B	0.40 (1)	0.44 (2)	0.40 (2)	0.52 (2)	0.56 (2)

1974). Initial fractional coordinates were obtained from Horiuchi and Sawamoto (1981) and all atoms were refined with anisotropic temperature factors. Occupancy parameters for the three octahedral sites were adjusted subject to a constraint of total chemistry. There is no evidence for octahedral vacancies as observed by Horiuchi and Sawamoto (1981). An isotropic extinction correction using the Lorentzian distribution of Becker and Coppens (1974) was refined for all crystals. This parameter was significant for two of the crystals, the iron-free composition and the one with Fe/(Fe+Mg)=0.25. Final values for the R factors and the goodness of fit (GOF) are listed in Table 1. The refined parameters, which include positions, occupancies and equivalent isotropic temperature factors, are presented in Table 2. Listings of observed and calculated structure factors, and standard deviations of the observed F's are available from the first author.

Discussion and Conclusions

Effects of Iron on the Wadsleyite Crystal Structure

Several features of the β-phase structure can be observed in Fig. 2. Chains of alternating M1 and M2 edge-shared octahedra are stacked parallel to *b*, and are adjacent to double chains of M3 octahedra that are parallel to *a*. The Si_2O_7 dimers, oriented parallel to *b*, are corner-linked to these octahedral elements.

Bond distances and angles for the five samples are

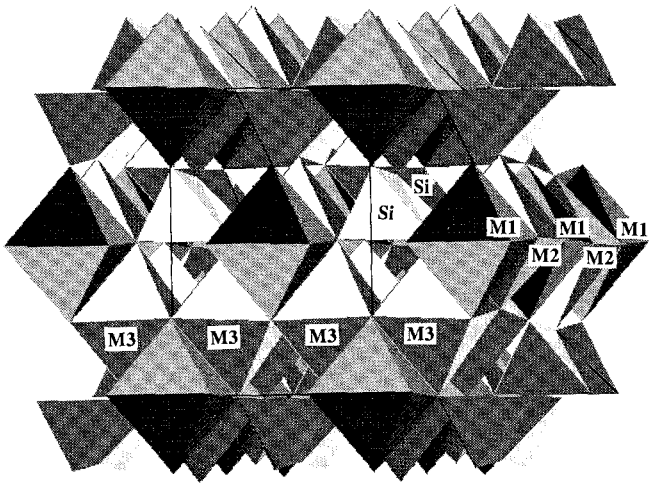

Fig. 2. A polyhedral representation of the wadsleyite (β-$(Mg,Fe)_2SiO_4$) structure with the α axis horizontal and the *c* axis vertical. Chains of alternating, edge-sharing M1 and M2 octahedra run parallel to *b*, while double chains of M3 octahedra are parallel to α. Tetrahedral Si_2O_7 dimers are corner linked to these octahedral chains

Table 3. Bond distances for iron-bearing wadsleyite

Distance	Fe00	Fe08	Fe16	Fe25	Fe40
Si tetrahedron					
Si-O2	1.703 (1)	1.701 (1)	1.701 (1)	1.702 (1)	1.704 (1)
Si-O3	1.639 (1)	1.639 (1)	1.638 (1)	1.636 (2)	1.639 (2)
Si-O4 [2][a]	1.635 (1)	1.634 (1)	1.632 (1)	1.635 (1)	1.636 (1)
mean	1.653	1.652	1.651	1.652	1.654
O2-O3	2.754 (1)	2.752 (1)	2.749 (1)	2.747 (2)	2.747 (2)
O2-O4 [2]	2.641 (1)	2.639 (1)	2.640 (1)	2.644 (2)	2.649 (2)
O3-O4 [2]	2.710 (1)	2.707 (1)	2.706 (1)	2.705 (2)	2.709 (2)
O4-O4	2.724 (1)	2.726 (1)	2.718 (2)	2.722 (3)	2.725 (2)
M1 octahedron					
M1-O3 [2]	2.113 (1)	2.120 (1)	2.124 (1)	2.132 (2)	2.140 (2)
M1-O4 [4]	2.047 (1)	2.049 (1)	2.057 (1)	2.061 (1)	2.073 (1)
mean	2.069	2.073	2.080	2.085	2.095
O3-O4 [4][b]	3.040 (1)	3.050 (1)	3.061 (1)	3.075 (2)	3.088 (2)
O3-O4 [4]	2.840 (1)	2.843 (1)	2.849 (1)	2.851 (2)	2.866 (2)
O4-O4 [2][b]	2.968 (1)	2.977 (2)	2.994 (2)	2.995 (3)	3.014 (2)
O4-O4 [2]	2.818 (1)	2.816 (2)	2.822 (2)	2.833 (3)	2.845 (3)
M2 octahedron					
M2-O1	2.052 (1)	2.037 (2)	2.044 (2)	2.052 (3)	2.061 (3)
M2-O2	2.090 (1)	2.099 (2)	2.101 (2)	2.110 (3)	2.111 (3)
M2-O4 [4]	2.088 (1)	2.091 (1)	2.097 (1)	2.100 (1)	2.105 (1)
mean	2.083	2.076	2.089	2.087	2.099
O1-O4 [4][b]	2.793 (1)	2.791 (1)	2.799 (1)	2.807 (2)	2.815 (2)
O2-O4 [4]	3.085 (1)	3.087 (2)	3.094 (2)	3.102 (2)	3.107 (2)
O4-O4 [2]	2.915 (1)	2.920 (2)	2.915 (2)	2.923 (3)	3.014 (2)
O4-O4 [2][b]	2.968 (1)	2.977 (2)	2.994 (2)	2.995 (3)	3.014 (2)
M3 octahedron					
M3-O1 [2]	2.025 (1)	2.027 (1)	2.033 (1)	2.043 (1)	2.050 (1)
M3-O3 [2]	2.119 (1)	2.122 (1)	2.125 (1)	2.132 (1)	2.134 (1)
M3-O4 [2]	2.123 (1)	2.132 (1)	2.134 (1)	2.139 (1)	2.141 (1)
mean	2.089	2.094	2.097	2.105	2.108
O1-O1[b]	2.892 (1)	2.904 (1)	2.907 (1)	2.908 (1)	2.917 (1)
O1-O3 [2][b]	3.001 (1)	3.001 (1)	3.011 (1)	3.033 (2)	3.036 (2)
O1-O4 [4][b]	2.793 (1)	2.791 (1)	2.799 (1)	2.807 (2)	2.815 (2)
O1-O4 [2]	3.105 (1)	3.124 (2)	3.122 (3)	3.126 (3)	3.123 (3)
O3-O3	2.847 (1)	2.854 (1)	2.858 (1)	2.860 (1)	2.872 (1)
O3-O4 [4][b]	3.040 (1)	3.050 (1)	3.061 (1)	3.075 (2)	3.088 (2)
O3-O4 [2]	2.915 (1)	2.920 (2)	2.923 (2)	2.935 (2)	2.939 (2)

[a] Numbers in square brackets indicate the multiplicity of the bond
[b] Edge shared between two octahedra.

given in Tables 3 and 4, respectively. Within the Si tetrahedron, both distances and angles are unaffected by substituting Fe for Mg. The mean M–O distances and octahedral volumes increase with iron content, however, as expected. The variation in lattice constants with iron content is linear, as illustrated in Fig. 3.

Iron orders into the three distinct octahedra, with enrichment in the sequence M3 > M1 > M2. This fractionation correlates with neither polyhedral volume nor with the polyhedral distortion parameters of Robinson et al. (1971); however, it is inversely correlated with the site potential calculated by Smyth (1987). Elongations of the *a* and *c* axes due to iron substitution (comparing unit-cell parameters of the samples with 0 and 40% Fe) are approximately 0.8%, while that of *b* is approximately 0.5%. This anisotropy reflects the relative depletion of iron in M2 relative to M1 and M3. The M2 octahedron helps to dictate the *b* dimension through M1–M2 octahedral chains.

There are no obvious structural features that might explain the observed Fe/(Fe+Mg) limit of wadsleyite. Figure 2 shows a three-dimensional view of the structure. The Si and three Mg–Fe cation polyhedra are nearly regular and remain well behaved at all compositions. No unusual trends are observed in bond distances or angles with increasing iron content, nor are there any obviously anomalous features in the sample with Fe/(Fe+Mg) = 0.40. It appears, therefore, that the stability of this iron-bearing wadsleyite must be understood relative to the olivine and silicate spinel forms of Mg–Fe orthosilicate.

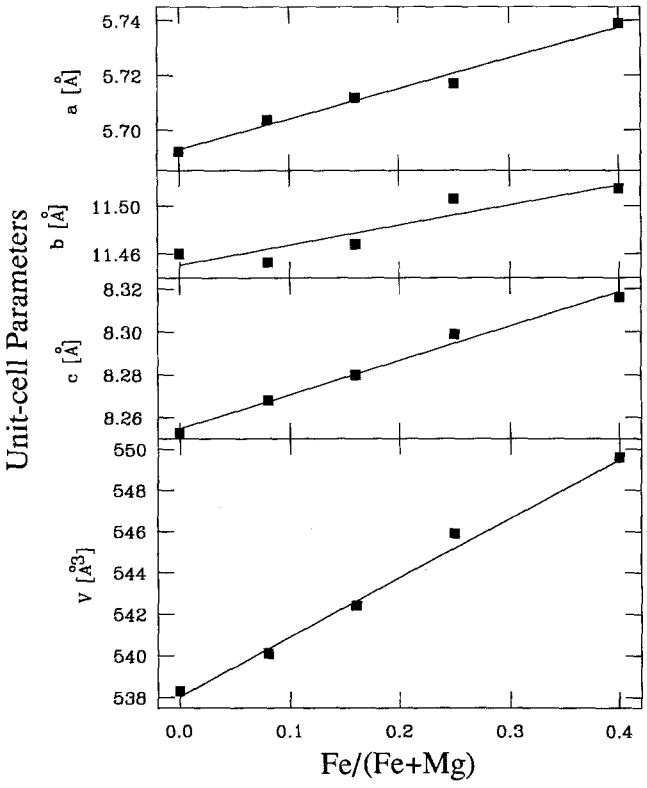

Fig. 3. Orthorhombic unit-cell parameters for β-$(Mg,Fe)_2SiO_4$ vary linearly as a function of iron content

Implications of Synthesis of β-$(Mg_{0.6}Fe_{0.4})_2SiO_4$

The unexpected synthesis of a wadsleyite sample with Fe/(Fe+Mg)=0.40 – a composition significantly more iron-rich than the limit of about 0.25 extrapolated from phase equilibria data at lower temperature (Akaogi et al. 1989) – raises serious questions about proposed phase equilibria for the system $Mg_2SiO_4-Fe_2SiO_4$ at mantle conditions. Experiments and calculations of the wadsleyite stability field (e.g., Katsura and Ito 1989; Akaogi et al. 1989; Fei et al. 1991) would place the synthesis conditions of the present sample (15.2 GPa and 1700° C) well within the silicate spinel stability field (Fig. 1). For example, Katsura and Ito (1989) obseved a mixture of β-$(Mg_{0.78}Fe_{0.22})_2SiO_4$ plus γ-$(Mg_{0.67}Fe_{0.33})_2SiO_4$ from a $(Mg_{0.7}Fe_{0.3})_2SiO_4$ starting composition at 15 GPa and 1600° C, while they found single phase silicate spinel at 13 GPa and 1600° C for more iron-rich samples.

The conditions of the present synthesis differed from previous experiments in three significant ways. First, the temperatures used, 1700 and 1800° C, were significantly higher than those for most earlier experiments, which were generally done at 800 to 1400° C, with a few runs (Katsura and Ito 1989) at 1600° C. It is possible that the width of the wadsleyite phase expands more rapidly with temperature than calculated using current best estimates of thermochemical data (Fei et al. 1991). This situation would require a revision of the thermochemical

Table 4. Bond angles for iron-bearing wadsleyite

Angle	Fe00	Fe08	Fe16	Fe25	Fe40
Si tetrahedron					
O2-Si-O3	110.91 (5)	110.94 (8)	110.84 (7)	110.77 (10)	110.48 (10)
O2-Si-O4 [2][a]	104.56 (3)	104.61 (5)	104.72 (5)	104.83 (7)	104.90 (7)
O3-Si-O4 [2]	111.75 (3)	111.59 (5)	111.68 (5)	111.62 (7)	111.66 (7)
O4-Si-O4	112.83 (5)	113.05 (7)	112.77 (7)	112.75 (9)	112.79 (9)
M1 octahedron					
O3-M1-O4 [4]	93.89 (2)	94.03 (4)	94.10 (3)	94.32 (5)	94.28 (5)
O3-M1-O4 [4]	86.11 (2)	85.97 (4)	85.90 (3)	85.68 (5)	85.79 (5)
O4-M1-O4 [2]	92.97 (3)	93.20 (6)	93.38 (5)	93.18 (8)	93.31 (8)
O4-M1-O4 [2]	86.11 (2)	86.80 (6)	86.62 (5)	86.82 (8)	86.69 (8)
M2 octahedron					
O1-M2-O4 [4]	84.83 (2)	85.06 (4)	85.04 (3)	85.08 (5)	85.03 (4)
O2-M2-O4 [4]	95.17 (2)	94.94 (4)	94.96 (3)	94.92 (5)	94.97 (4)
O4-M2-O4 [2]	88.49 (5)	88.34 (5)	88.05 (5)	88.20 (8)	87.67 (7)
O4-M2-O4 [2]	90.59 (3)	90.81 (5)	91.10 (5)	90.95 (7)	91.47 (7)
M3 octahedron					
O1-M3-O1	91.17 (2)	91.52 (3)	91.26 (3)	90.76 (4)	90.71 (4)
O1-M3-O3 [2]	92.81 (2)	92.67 (3)	92.78 (2)	93.15 (4)	93.03 (4)
O1-M3-O4 [2]	84.61 (4)	84.26 (6)	84.35 (6)	84.30 (8)	84.56 (7)
O1-M3-O4 [2]	96.91 (4)	97.36 (6)	96.99 (6)	96.71 (9)	96.29 (6)
O3-M3-O3	84.45 (4)	84.52 (5)	84.53 (5)	84.27 (7)	84.56 (7)
O3-M3-O4 [2]	91.56 (3)	91.61 (5)	91.90 (5)	92.11 (6)	92.49 (6)
O3-M3-O4 [2]	86.83 (3)	86.69 (5)	86.69 (5)	86.83 (6)	86.95 (5)
O3-O2-O3	170.53 (6)	170.6 (1)	170.62 (9)	170.55 (13)	170.86 (13)
Si-O2-Si	121.89 (7)	121.84 (11)	121.72 (11)	121.78 (15)	121.19 (15)

[a] Numbers in square brackets indicate the multiplicity of the angle

Table 5. Polyhedral parameters for iron-bearing wadsleyite

Parameter	Fe00	Fe08	Fe16	Fe25	Fe40
M1, V	11.727 (4)	11.778 (8)	11.901 (8)	11.984 (11)	12.200 (10)
QE[a]	1.0046 (1)	1.0051 (2)	1.0053 (2)	1.0056 (3)	1.0057 (2)
AV	14.2	15.6	16.4	17.3	17.6
VS	2.2	2.2	2.2	2.2	2.2
M2, V	11.943 (5)	11.976 (8)	12.056 (8)	12.144 (11)	12.230 (10)
QE	1.0056 (7)	1.0053 (10)	1.0054 (10)	1.0052 (14)	1.0056 (7)
AV	19.9	18.4	18.8	18.4	19.8
VS	2.1	2.1	2.1	2.1	2.1
M3, V	12.045 (4)	12.112 (5)	12.189 (5)	12.316 (7)	12.407 (5)
QE	1.0063 (3)	1.0069 (4)	1.0066 (4)	1.0065 (5)	1.0062 (4)
AV	20.6	22.5	21.6	21.6	20.5
VS	2.0	2.1	2.1	2.1	2.1
Si, V	2.306 (1)	2.303 (2)	2.298 (2)	2.302 (3)	2.303 (3)
QE	1.0036 (6)	1.0035 (9)	1.0034 (9)	1.0033 (13)	1.0032 (17)
AV	14.5	14.1	13.7	13.1	13.0
VS	3.8	3.8	3.8	3.8	3.8
O1, VS	2.0	2.0	2.0	2.0	2.0
O2, VS	2.0	2.0	2.0	2.0	2.0
O3, VS	1.9	1.9	1.9	1.9	1.9
O4, VS	2.0	2.0	2.0	2.0	2.0

[a] QE and AV stand for the quadratic elongation and angle variance parameters, respectively, of Robinson et al. (1971). VS stands for the valence sum of Brown (1981)

data base, and an internally consistent set of data reproducing the phase equilibria and calorimetric determinations of enthalpies of phase transitions and solid solution mixing properties might be achievable.

Second, the runs were of longer duration 3 h instead of the 10 to 20 min typical of previous experiments. This longer duration, coupled with the higher temperature, might suggest that equilibrium was more likely to have been attained in our experiments. However, the general consistency of previous experiments with each other, the presence of several reversals in those studies, and the agreement of the phase diagram calculated from thermochemical data with the measured equilibria (Fei et al. 1991), give no hint of any significant disequilibrium in previous studies. Nevertheless, the new results point to the great need for fully reversed phase equilibrium studies, despite the recognized difficulty of performing such reversals.

Third, and pointing toward a possible source of disequilibrium in our studies, was the nature of the starting materials. Whereas most of the previous work used an olivine solid solution as starting material, our runs, aimed initially at crystal growth and not phase equilibria, used a mechanical mixture of forsterite and fayalite, ground together in the desired proportions. It is possible that wadsleyite may have nucleated as the stable phase in the Mg_2SiO_4 grains, while spinel nucleated in Fe_2SiO_4. If the specimen then homogenized by diffusion, with beta-gamma phase transformation being slow, the wadsleyite grains could have grown at the expense of the spinel, resulting in a homogenous beta-phase final product. This would have some implications, well worth exploring, for relative diffusion rates in the two structures.

In any case, the synthesis of a single crystal of wadsleyite that is significantly more iron-rich than any previously reported gives reason to reconsider critically the $Mg_2SiO_4-Fe_2SiO_4$ phase diagram. If wadsleyite with $Fe/(Fe+Mg)=0.4$ is indeed stable under conditions near 15 GPa and 1700° C, then the beta stability field may be greatly expanded and all three two-phase fields ($\alpha+\beta$, $\alpha+\gamma$, and $\beta+\gamma$) must be significantly altered. These modifications, in turn, would significantly change calculations of Fe–Mg partitioning in the mantle and alter the mineralogy needed to produce the seismic characteristics of the 400 km discontinuity.

Thermodynamic Implications of Fe–Mg Ordering in Wadsleyite

It is, at first glance, somewhat surprising that a significant degree of Fe–Mg ordering between M1, M2, and M3 sites occurs in single crystals quenched from temperatures as high as 1800° C. Since cation distributions have not been determined from the powders synthesized in previous experiments, we do not know whether the extent of ordering observed is in fact greater in our samples – a situation possible because of their longer equilibration times. Thus we can not say whether the present samples, for $Fe/(Fe+Mg)\leq 0.25$, represent structural and thermodynamic states that are the same or different from those of samples used in previous equilibria and calorimetry (Akaogi et al. 1989). Furthermore, because cation distributions in spinels are generally not quenchable from temperatures above 1100° C (Wood et al. 1986), the observed state of order in wadsleyite could be characteristic of a temperature much lower than the 1700 to 1800° C synthesis conditions. These uncertain-

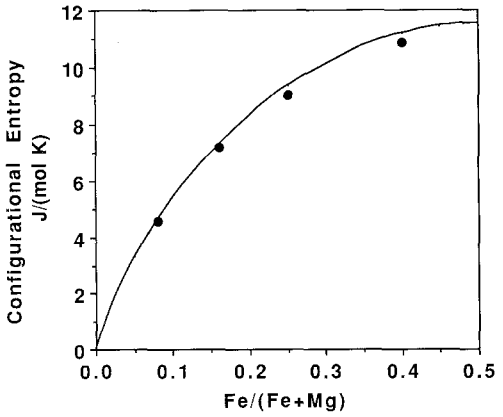

Fig. 4. Configurational entropy versus Fe/(Fe+Mg) for synthetic wadsleyites. The solid curve represents the configuration entropy for Fe–Mg disordered wadsleyites, while the four points are calculated configurational entropies for the partially ordered synthetic samples of this study

ties, plus the question raised above whether the most iron-rich wadsleyite represents a stable phase equilibrium, makes it premature to develop a detailed thermodynamic model incorporating the ordering energetics.

Nevertheless, it is enlightening to address the thermodynamic consequences of ordering more qualitatively. One might first ask to what extent the degree of ordering seen would decrease the configurational entropy of the beta phase. A completely random $Mg_2SiO_4-Fe_2SiO_4$ solid solution, with Fe/(Fe+Mg)=N, would have configurational entropy:

$$S_{\text{conf, disordered}} = -2R[N\ln N+(1-N)\ln(1-N)].$$

If one treated the three distinct M sites separately, then per formula unit $(Mg_{1-N}Fe_N)_2SiO_4$, there would be 0.5 M1 sites (with Fe/(Fe+Mg)=x from the structure refinement), 0.5 M2 sites (with Fe/(Fe+Mg)=y) and 1.0 M3 site (with Fe/(Fe+Mg)=z). The configurational entropy per mole $(Mg_{1-N})_2SiO_4$ would then be:

$$S_{\text{conf, partly ordered}}$$
$$= -R[0.5\,x\ln x+0.5(1-x)\ln(1-x)+0.5\,y\ln y$$
$$+0.5(1-y)\ln(1-y)-z\ln z+(1-z)\ln(1-z)].$$

These two functions are compared in Fig. 4. For the four samples synthesized, one sees the configurational entropy decreases only very slightly from its maximum value for total disorder, despite what might at first be judged to be significant ordering. This is because a very substantial amount of disorder over the three sites remains, and the configurational entropy, because of its intrinsically logarithmic form, increases steeply for the initial disordering of a fully ordered phase, but changes only slowly for small degrees of ordering of a fully disordered material. Thus the extent of ordering seen in the single crystals, whether representative of 1800° C, or a lower temperature, does not decrease the entropy much, and is not unreasonable for a high-temperature material. It may, nonetheless, have a more significant effect on the partial molar thermodynamic parameters and on activity-composition relations.

Although the crystallographic data could, in principle, be used to calculate apparent distribution coefficients and apparent equilibrium constants for Fe–Mg partitioning among the three sites, the thermodynamic significance of such a calculation would be in doubt because of the uncertainties relating to the attainment of equilibrium and the quenchability of cation distributions discussed above. Much more detailed study is needed to determine the energetics of order-disorder in these materials. Annealing studies at lower temperatures, from which cation distribution could probably be preserved during quench, would be appropriate. It would also be valuable to try to reproduce the synthesis of $(Mg_{0.6}Fe_{0.4})_2SiO_4$ wadsleyite using a homogeneous olivine solid solution under our experimental conditions. Such work is planned for the future.

Acknowledgements. The synthesis of single crystals was performed in the Stony Brook High-Pressure Laboratory, which is jointly sponsored by the NSF Center for High Pressure Research and the State University of New York. Crystallographic studies at the Geophysical Laboratory are supported by NSF grant EAR89-16709 and the Carnegie Institution of Washington. Thermodynamic analysis at Princeton was aided by the NSF Science and Technology Center for High-Pressure Research. We have benefited from the comments and reviews of Y. Fei, H.K. Mao, R.J. Hemley, C. Meade, and T. Gasparik.

References

Akaogi M, Ito E, Navrotsky A (1989) Olivine–modified spinel–spinel transitions in the system $Mg_2SiO_4-Fe_2SiO_4$: Calorimetric measurements, thermochemical calculation, and geophysical application. J Geophys Res 94:15671–15685

Becker P, Coppens P (1974) Extinction within the limit of validity of the Darwin transfer equations. General formalisms for primary and secondary extinction and their application to spherical crystals. Acta Crystallogr A 30:129–147

Brown ID (1981) The bond-valence method: An empirical approach to chemical structure and bonding. In: O'Keeffe M, Navrotsky A (eds) Structure and bonding in crystals, vol II. Academic Press, New York, pp 1–30

Burnham CW (1966) Computation of absorption corrections, and the significance of end effects. Am Mineral 51:159–167

Downs JW (1989) Possible sites for protonation in β-Mg_2SiO_4 from an experimentally derived electrostatic potential. Am Mineral 74:1124–1129

Fei Y, Mao H-K, Mysen BO (1991) Experimental determination of element partitioning and calculation of phase relations in the MgO–FeO–SiO_2 system at high pressure and high temperature. J Geophy Res 96:2157–2169

Finger LW, Prince E (1975) A system of Fortran IV computer programs for crystal structure computations. NBS technical note 854, Nat. Bur. Stand. (US), p 128

Hazen RM, Zhang J, Ko J (1990) Effects of Fe/Mg on the compressibility of synthetic wadsleyite: β-$(Mg_{1-x}Fe_x)_2SiO_4$ ($X \leq 0.25$). Phys Chem Minerals 17:416–419

Horiuchi H, Sawamoto H (1981) β-Mg_2SiO_4: single crystal X-ray diffraction study. Am Mineral 66:568–575

Katsura T, Ito E (1989) The system $Mg_2SiO_4-Fe_2SiO_4$ at high pressures and temperatures: Precise determination of stabilities of olivine, modified spinel, and spinel. J Geophys Res 94:15663–15670

Lehmann MS, Larsen FK (1974) A method for location of the peaks in step-scan-measured Bragg reflexions. Acta Crystallogr A 30:580–584

Moore PB, Smith JV (1970) Crystal structure of β-Mg_2SiO_4: Crystal-chemical and geophysical implications. Phys Earth Planet Inter 3:166–177

Morimoto N, Akimoto S, Koto K, Tokonami M (1969) Modified spinel, beta-manganous orthogermanate: stability and crystal structure. Science 165:586–588

Ralph R, Finger LW (1982) A computer program for refinement of crystal orientation matrix and lattice constants from diffractometer data with lattice symmetry constraints. J Appl Crystallogr 15:537–539

Ringwood AE, Major A (1966) Synthesis of Mg_2SiO_4–Fe_2SiO_4 spinel solid solutions. Earth Planet Sci Lett 1:241–245

Robinson K, Gibbs GV, Ribbe PH (1971) Quadratic elongation: A quantitative measure of distortion in coordination polyhedra. Science 172:567–570

Smyth JR (1987) β-Mg_2SiO_4: A potential host for water in the mantle? Am Mineral 72:1051–1055

Wood BJ, Kirkpatrick RJ, Montez B (1986) Order-disorder phenomena in $MgAl_2O_4$ spinel. Am Mineral 71:999–1006